

Wavelength monitor based on two single-quantum-well absorbers sampling a standing wave pattern

H. L. Kung, D. A. B. Miller, P. Atanackovic,^{a)} C. C. Lin,^{b)} J. S. Harris, Jr.,^{b)} L. Carraresi,^{c)} J. E. Cunningham,^{d)} and W. Y. Jan^{d)}

Edward L. Ginzton Laboratory, Solid State and Photonics Laboratory, 450 Via Palou, Stanford University, Stanford, California 94305-4085

(Received 7 January 2000; accepted for publication 7 April 2000)

We demonstrate a wavelength monitor and a two-wavelength detector based on two single-quantum-well absorbers that sample a standing wave created by a distributed Bragg reflector. As a wavelength monitor, our device is power independent over a 15 dB range. Wavelength discrimination is linear over a 12 nm range. © 2000 American Institute of Physics.

[S0003-6951(00)04122-X]

The recent growth in wavelength division multiplexing has increased the demand for easy-to-integrate wavelength-sensitive photodetectors and wavelength monitors. Various devices have been proposed for wavelength-sensitive photodetectors, including Fabry–Perot resonator devices,¹ tunable filters integrated with a photodetector,² and Mach–Zehnder designs for wavelength demultiplexing.³ A class of devices based on thin absorbers in standing waves was proposed⁴ and one such device, a detector capable of rejecting a specific wavelength, was demonstrated.⁵ Wavelength monitors are necessary to monitor channel characteristics and system performance. Traditional grating spectrometers, wavemeters, concatenated fiber gratings,⁶ y-branch integrated monitors,⁷ and dual metal–semiconductor–metal (MSM) detectors with different finger spacing,⁸ have been demonstrated for wavelength monitoring.

We demonstrate a device that contains two thin-absorber photodetectors at different points in a standing wave. Our device can function as a wavelength monitor, a two-wavelength detector, or a detector that rejects a single, selected wavelength. It is a surface-normal device that could be readily integrated with silicon electronics or made into dense arrays. Our device samples the standing wave pattern; thus only a small fraction of the incoming signal is absorbed. The light that is not absorbed is reflected and can be reused. Due to the device structure, operation is relatively insensitive to temperature changes.

The device structure is shown in Fig. 1. An incident light beam is reflected by a distributed Bragg reflector (DBR) and a standing wave is created in the device. The device has an antireflection coating on the top surface; thus it is not a Fabry–Perot resonator. The thin absorbers sample the standing wave pattern. Figure 1 shows the extreme case where one

absorber is placed at a null of the standing wave while the other is placed at a peak. The peaks and nulls of the standing wave shift position as the wavelength changes. If an absorber lies at a null of the standing wave then there is no absorption by that absorber. Conversely, if the absorber is at a peak, the absorption will be a maximized. Thus, as the wavelength of light varies, the absorption at each absorber also varies. In our device we used quantum wells as the absorbers since they are only $\sim\lambda/25$ thick.

The signals from the two photodiodes can be combined in a normalized differential, “ $(A-B)/(A+B)$ ” fashion (where A is the signal from the top photodiode and B is the signal from the bottom photodiode) to make a wavelength monitor that is power independent, and we have demonstrated this operation. In another mode one may detect two wavelengths simultaneously and independently by choosing one wavelength to have a node at the bottom photodiode while the other has a node at the top photodiode. The device detects λ_1 while rejecting λ_2 and vice versa. With appropri-

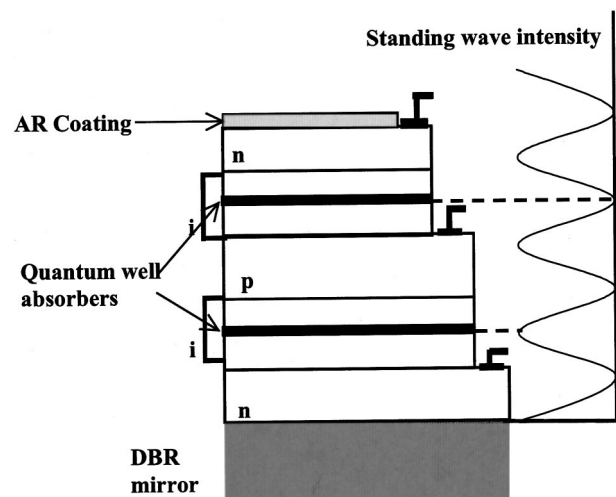


FIG. 1. Schematic of the device with a standing wave for a single wavelength with a zero phase change at the mirror. Mesas are etched to the p and the bottom n regions. Contacts are then placed on the top n, p, and bottom n regions. The contacts are used to extract the photocurrent from the two quantum wells and for reverse biasing the two diodes.

^{a)}On leave from Defense Science and Technology Organization Adelaide, Australia.

^{b)}Solid State and Photonics Laboratory, Center for Intergrated Systems, Stanford University, Stanford CA 94305-4090.

^{c)}Instituto Nazionale di Fisica della Materia, Dipartimento di Fisica and Laboratorio Europeo Spettroscopie Non-lineari (LENS), Univerisita' di Firenze, Largo E.Fermi 2, 50125 Firenze—Italy.

^{d)}Bell Laboratories, Lucent Technologies, 101 Crawfords Corner Road, Holmdel, NJ 07733.

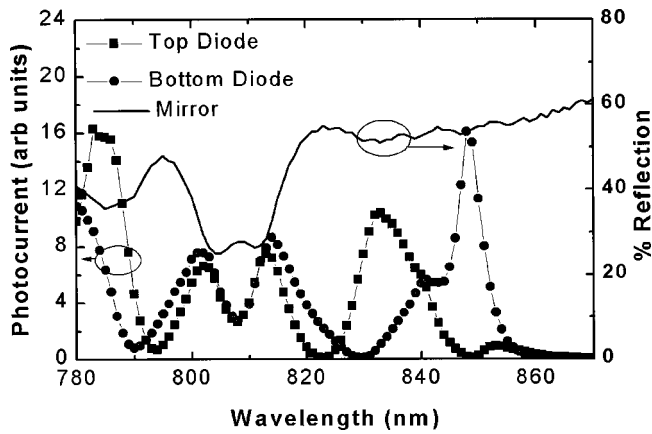


FIG. 2. Photocurrent spectrum from the top and bottom quantum wells are shown on the left axis. The mirror reflection is shown on the right axis.

ate spacer thickness, the rejection ratio is maximized and no postprocessing of the electrical outputs is necessary.

In general, two photodiodes give two independent pieces of information. For example, we can determine both wavelength and power of a signal simultaneously. Alternatively, we can measure power at two different known wavelengths.

The device was grown by solid-source molecular beam epitaxy (MBE) on an *i* GaAs (001) wafer. The device is an *n-i-p-i-n* structure grown on a DBR mirror. The DBR was grown with 7.5 pairs of AlAs/Al_{0.13}Ga_{0.87}As and a GaAs cap layer. The wafer was removed from the growth chamber to measure the reflectivity. The reflectivity was then corrected by adding a GaAs spacer and the remaining seven pairs of AlAs/Al_{0.13}Ga_{0.87}As were grown. Each absorber is a single 95 Å GaAs/Al_{0.4}Ga_{0.6}As quantum well. In addition to the quantum well, each *i* region consists of a transparent superlattice of alternating pairs of 20 Å GaAs/20 Å Al_{0.4}Ga_{0.6}As, which acts as a suitable substrate for growing a single quantum well,⁹ and a region of Al_{0.4}Ga_{0.6}As. Both *n* regions were doped at $\sim 1.4 \times 10^{18} \text{ cm}^{-3}$; the bottom *n* region has a thickness of 0.5 μm and the top *n* region has a thickness of 0.3 μm. The *p* region was doped at $\sim 2 \times 10^{18} \text{ cm}^{-3}$ and has a thickness of 0.5 μm. The temperature during growth of the *p* region was lowered to 525 °C to decrease dopant diffusion.¹⁰ Standard photolithography and wet chemical etching were used to make 300 and 600 μm square mesas. A Si₃N₄ antireflection coating was deposited on top of the mesas and metal ring contacts were made to the *p* and both *n* regions, followed by wire bonding.

The diodes were reverse biased at 2.5 V and the photocurrent from the two diodes was simultaneously measured while under illumination from a tunable Ti³⁺:Al₂O₃ laser. The signal from each diode is shown in Fig. 2. With better thickness control during growth we would have the case shown in Fig. 1 where there is a null at 830 nm for the bottom detector and a peak at 830 nm for the top detector. The top diode rejects 823 nm and is a strong detector for 833 nm. There is a 22 dB rejection ratio between these two wavelengths. The bottom diode on the other hand is a strong detector of 848 nm and rejects 830 nm with a rejection ratio of 22 dB. The top photodiode has a peak external quantum efficiency of 2.1% (responsivity of 0.015 A/W). The bottom photodiode has a peak external quantum efficiency of 4.2%

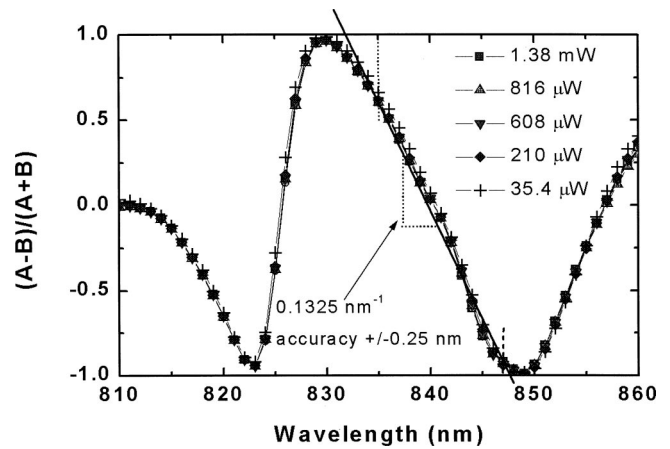


FIG. 3. $(A-B)/(A+B)$ where *A* is the top diode's photocurrent and *B* is the bottom diode's photocurrent, for different power levels from 35.4 μW to 1.38 mW. A straight line approximation from 835 to 847 nm has a slope of 0.1325 nm^{-1} .

at the exciton peak (responsivity of 0.029 A/W). For the bottom diode there is a nonzero amount of photocurrent at 790 nm. This is most likely because the superlattice is not completely transparent, with some absorption caused by the Urbach tail of the superlattice. The thickness of the superlattice is 200 times that of the quantum well; thus a weak band-tail absorption coefficient can give relatively significant absorption overall. There is a dip in the photocurrent at 823 nm caused by an unintended null in the DBR mirror reflectivity at 823 nm, as seen in Fig. 2.

To create a wavelength monitor we measured the photocurrents from the two diodes simultaneously, recording a differential photocurrent [$“(A-B)/(A+B)”$]. The results for various power levels are shown in Fig. 3. As seen in Fig. 3 the device is power insensitive over the tested range of 35.4 μW to 1.38 mW. The device can be used as a wavelength-sensitive detector from 835 to 847 nm. In that region the response can be fit by a line with a slope of 0.1325 nm^{-1} . The R^2 value of the linear fit is 0.99. Using this linear approximation an accuracy of $\pm 0.25 \text{ nm}$ is achieved. The accuracy is much better if we use a look-up table.

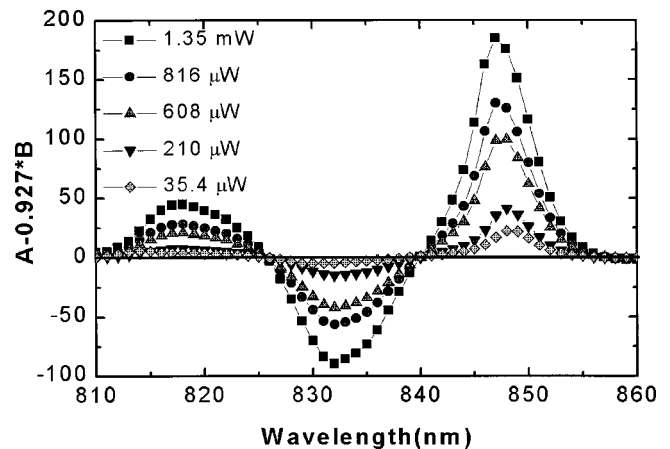


FIG. 4. An example of how postprocessing can be used to reject a single wavelength. In this case the wavelength was 840 nm. The weighting that is needed is $\text{signal} = A - 0.927 \cdot B$. The intensity of the signal at other wavelengths is proportional to power.

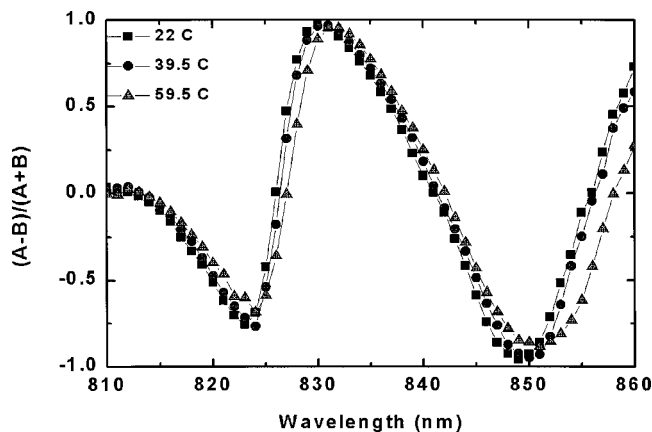


FIG. 5. $(A-B)/(A+B)$ vs wavelength for different temperatures.

If the spacer thicknesses are not optimized, the electrical signals may be postprocessed to extract desired information. The response of each photodiode with respect to wavelength can be viewed as a filter acting on the incoming light. Given the filter response of each diode it is possible, to weigh the signals and combine them to reject any single wavelength. Proper weighing to reject 840 nm is shown in Fig. 4. With the rejection of a single wavelength there is another wavelength that is also rejected due to the periodic nature of the two filters. The intensities of two known wavelengths can be determined by this method. By rejecting one of the wavelengths of interest we can determine the power at the other wavelength, and vice versa.

It is important that wavelength monitors are temperature insensitive. The two main effects that temperature has on our device are changes in refractive index and movement of the absorption edge. We heated the device from 22 to 59.5 °C and measured $(A-B)/(A+B)$ signals at a fixed power level. Figure 5 shows the results at three temperatures. The device has a temperature shift of $0.27 \text{ \AA}/^\circ\text{C}$, in the wavelength range from 830 to 845 nm. At larger wavelengths than 845

nm the temperature shift is much larger due to exciton and band gap effects. The relatively small shifts with respect to temperature can be attributed to the device composition ($\text{Al}_{0.4}\text{Ga}_{0.6}\text{As}$) and operating far from its band edge.

In conclusion, we have demonstrated a device based on two absorbers in a standing wave that has many possible functions depending on how the electrical output of the two photodiodes are combined. It would be straightforward to integrate the electrical output of our monitor into a feedback loop to stabilize the wavelength of a diode laser. We have also demonstrated a detector that can reject any single wavelength. This idea could be extended to many photodetectors. The number of photodetectors determines the number of independent pieces of information that can be determined. The design could be improved by operating in a wavelength range that is farther from the exciton wavelength, where the device would not be as sensitive to temperature fluctuations.

This work was supported by Grant No. MDA972-98-1-0002 from DARPA and a subaward from the University of New Mexico. H.L.K. was funded by an NSF graduate fellowship and a Lucent Technologies GRPW grant.

- ¹S. Y. Hu, J. Ko, and L. Coldren, *Appl. Phys. Lett.* **70**, 2347 (1997).
- ²K. W. Goossen, J. E. Cunningham, J. Santos, and W. Y. Jan, *Appl. Phys. Lett.* **62**, 3229 (1993).
- ³A. Tervonen, P. Poyhonen, S. Honkanen, and M. Tahkokorpi, *IEEE Photonics Technol. Lett.* **3**, 516 (1991).
- ⁴D. A. B. Miller, *IEEE J. Quantum Electron.* **30**, 732 (1994).
- ⁵L. Carraresi, E. A. DeSouza, D. A. B. Miller, W. Y. Jan, and J. E. Cunningham, *Appl. Phys. Lett.* **64**, 134 (1994).
- ⁶C. R. Giles, T. Strasser, K. Dryer, and Chris Doerr, *IEEE Photonics Technol. Lett.* **10**, 1452 (1998).
- ⁷B. Mason, S. P. DenBaars, and L. A. Coldren, *IEEE Photonics Technol. Lett.* **10**, 1085 (1998).
- ⁸E. Chen and S. Y. Chou, *Electron. Lett.* **32**, 1510 (1996).
- ⁹J. D. Ralston, E. C. Larkins, W. Rothemund, I. Esquivias, W. Weisser, J. Josenzweig, and J. Fleisser, *J. Cryst. Growth* **127**, 19 (1993).
- ¹⁰E. F. Schubert, *Delta-Doping of Semiconductors* (Cambridge University Press, Great Britain, 1996).